

## Preparation and Electrochemical Performance of CoOOH-Coated Ni<sub>0.8</sub>Mn<sub>0.2</sub>(OH)<sub>2</sub> Cathode Materials

Shouguang Yao<sup>1,\*</sup>, Dun Liu<sup>1,2</sup>, Fei Dou<sup>1,2</sup>, Jie Cheng<sup>2,3</sup>, Yusheng Yang<sup>2,3</sup>

<sup>1</sup> School of Energy and Power Engineering, Jiangsu University of Science and Technology, Zhenjiang, Jiangsu 212003, China

<sup>2</sup> Zhangjiagang Smartgrid Fanghua electrical energy storage research institute Co. Ltd., Zhangjiagang 215600, China

<sup>3</sup> Chilwee Power Co., Ltd., Huzhou 313100, China

\*E-mail: [zjyaosg@126.com](mailto:zjyaosg@126.com)

Received: 3 October 2020 / Accepted: 21 November 2020 / Published: 31 December 2020

---

CoOOH-coated Ni<sub>0.8</sub>Mn<sub>0.2</sub>(OH)<sub>2</sub> samples were prepared by chemical coprecipitation method, and the cobalt mass fractions were 2.5%, 5%, 7.5% and 10%. X-ray diffraction measurements showed that the samples were mainly composed of  $\beta$ -Ni(OH)<sub>2</sub>, and some of the CoOOH-coated samples contained a small amount of impurities. Scanning electron microscopy measurements showed the CoOOH attachment on the surface of the sample particles. Cyclic voltammetry results showed that CoOOH coated on the surface of the sample could reduce the difference between oxidation and reduction peak potentials and increase the oxygen evolution potential of the electrode. Constant current charge-discharge results showed that sample CoOOH=5% yielded the highest discharge specific capacity and the best cycle stability with a discharge specific capacity of 282 mAh·g<sup>-1</sup> at 100 mA·g<sup>-1</sup>. In the meantime, the discharge specific capacity of commercial  $\beta$ -Ni(OH)<sub>2</sub> was 270 mAh·g<sup>-1</sup>. When the sample CoOOH=5% was cycled at 800 mA·g<sup>-1</sup>, the discharge specific capacity did not decrease for 30 cycles, whilst other samples containing Co and commercial  $\beta$ -Ni(OH)<sub>2</sub> showed different degrees of discharge specific capacity. Several experimental results proved that the sample with CoOOH mass fraction of 5% had good multiplier property and could improve the cycling stability of nickel electrode.

---

**Keywords:** Chemical coprecipitation method; Coating; Rate capability; Cyclic stability

### 1. INTRODUCTION

Single liquid flow battery has become a new type of energy storage device with good development prospect due to its advantages, such as large energy storage scale, high cost performance, strong cycling ability and environmental protection. In 2007, Cheng Jie's group [1-3] presented a zinc-nickel single-liquid battery with a sintered nickel electrode as the positive electrode. This battery solves the problem of zinc dendrite by flowing the electrolyte and controlling zinc deposition/dissolution. The

electrolyte containing ZnO can stabilise the crystal structure of Ni(OH)<sub>2</sub> [4] and greatly improve the cycle life; however, the overall specific energy of the battery is decreased. The research team used several methods to improve its performance.

Nickel hydroxide, which is a positive electrode material, has a vital influence on the performance of nickel-based batteries (Ni/MH, Ni/Cd, Ni/Zn, Ni/Fe). The material generally has  $\alpha$ -Ni(OH)<sub>2</sub> and  $\beta$ -Ni(OH)<sub>2</sub> main crystal types [5].  $\alpha$ -Ni(OH)<sub>2</sub> has a high specific capacity but can be easily converted to  $\beta$ -Ni(OH)<sub>2</sub> in a strongly alkaline environment [6], which limits its application. The theoretical specific capacity of  $\beta$ -Ni(OH)<sub>2</sub> (289 mAh/g) is lower than that of  $\alpha$ -Ni(OH)<sub>2</sub> (482 mAh/g), but the former can work steadily and discharge in high power in alkaline environment. Domestic and foreign scholars have conducted some doping and coating modification treatments on  $\beta$ -Ni(OH)<sub>2</sub> to improve the performance of  $\beta$ -Ni(OH)<sub>2</sub>, [7-13].

Hou Xingang's group [14] prepared nanometre nickel hydroxide by precipitation transformation method and coated CoOOH with various contents by chemical precipitation method. The results showed that a structure of  $\beta$ -Ni(OH)<sub>2</sub> is preserved and w (CoOOH)=2.5% can be formed as a well-distributed conductive network on the surface of nickel hydroxide particles; these conditions lead to improved utilisation of active material. Xia Pan's group [15] prepared cobalt-coated nanometre nickel hydroxide samples by chemical coprecipitation under the action of ultrasound. The results of the charge–discharge performances of the testing batteries showed that Ni(OH)<sub>2</sub> sample exhibits good electrochemical properties with a specific discharge capacity of 358.6 mAh/g and a high discharging efficiency of 96.8% at the 404th cycle with a charge–discharge rate of 5C. Ni(OH)<sub>2</sub> sample doped with 3% Co in molar ratio has the best electrochemical characteristic. Hao Wenxiu's group [16] coated nickel hydroxide with cobalt hydroxide and ytterbium hydroxide. The results showed that the structure of  $\beta$ -Ni(OH)<sub>2</sub> is hexagonal, Co exists mainly in the form of Co<sup>2+</sup> with a small amount of Co<sup>3+</sup> and the atomic ratio of Co and Ni on the sample surface is more than 8:1. The samples coated with 2 wt% Yb(OH)<sub>3</sub> show the maximum discharge capacity and active material utilisation rate at 65 °C (0.2, 1, 3 C). He Xiangming's group [17] used ytterbium hydroxide, calcium phosphate and cobalt hydroxide to modify the surface of spherical Ni(OH)<sub>2</sub> to improve its high-temperature performance. The Yb/Co-coated spherical Ni(OH)<sub>2</sub> was prepared by coprecipitation of Co/Yb hydroxide on the surface of spherical Ni(OH)<sub>2</sub> from CoSO<sub>4</sub>, YbCl<sub>3</sub> and NaOH solutions. The Ca<sub>3</sub>(PO<sub>4</sub>)<sub>2</sub> and Co(OH)<sub>2</sub>-coated Ni(OH)<sub>2</sub> samples were prepared by precipitation of Ca<sub>3</sub>(PO<sub>4</sub>)<sub>2</sub> on the surface of spherical Ni(OH)<sub>2</sub>, followed by precipitation of Co(OH)<sub>2</sub> on its surface. The results showed that the two methods can effectively improve the high-temperature (60 °C) performance of spherical Ni(OH)<sub>2</sub>. By controlling crystallisation, Li Wen's group [18] coated the spherical nickel hydroxide with a layer of Yb(OH)<sub>3</sub> and studied the effects of different coating contents on the properties of the spherical nickel hydroxide coated with Yb(OH)<sub>3</sub> at room and high temperatures. The properties of the spherical nickel hydroxide coated with Yb(OH)<sub>3</sub> are reduced at room temperature, but the properties at high temperature are greatly improved. The results of 1C charge and discharge at 60 °C showed that the spherical nickel hydroxide with a coating volume of 2% (molar ratio) has the best high-temperature performance, and its high-temperature capacity retention rate can reach 92%. Lv Xiang's group [19] coated CoOOH on the surface of spherical Ni(OH)<sub>2</sub> particles by chemical precipitation method. Scanning electron microscopy (SEM) showed that CoOOH can adhere to the surface of Ni(OH)<sub>2</sub> particles. Tafel curve and electrochemical impedance spectroscopy showed that the

corrosion resistance and electrical conductivity of the material are optimised. In the meantime, the suitable coating amount of the material is 3%, and the retention rate of nickel electrode is 83.2% after 40 charge and discharge cycles of 0.2 C.

Previous literature showed that Mn-doped Ni(OH)<sub>2</sub> prepared by buffer solution method presents good electrochemical performance [20]. The discharge specific capacity can reach 271.8 mAh·g<sup>-1</sup> when the Mn content is 20 mol%. In the current study, Ni<sub>0.8</sub>Mn<sub>0.2</sub>(OH)<sub>2</sub> was surface-coated CoOOH based on the literature [20]. Ni<sub>0.8</sub>Mn<sub>0.2</sub>(OH)<sub>2</sub> was prepared by buffer solution method, and CoOOH was coated on the surface of Ni<sub>0.8</sub>Mn<sub>0.2</sub>(OH)<sub>2</sub> by chemical coprecipitation method. Compared with commercial Ni(OH)<sub>2</sub>, the best electrochemical performance was found when the cobalt mass fraction was 5%.

## 2. EXPERIMENTAL SECTION

### 2.1. Material Synthesis

Ni<sub>0.8</sub>Mn<sub>0.2</sub>(OH)<sub>2</sub> was prepared by buffer solution method [21,22]. Firstly, a buffer solution was prepared by dissolving 5.4 g of ammonium chloride in distilled water. Approximately 35 mL of ammonia water was added to the mixture until a constant volume of 100 mL was obtained. The pH of the solution was around 10. Secondly, appropriate amounts of NiSO<sub>4</sub>·6H<sub>2</sub>O and MnSO<sub>4</sub>·H<sub>2</sub>O were dissolved in 200 mL of distilled water on the basis of the molar ratios of Ni and Mn at 80:20; thus, solution 1 was prepared. Solution 2 was obtained by dissolving 16 g NaOH in 200 mL of deionised water. Thirdly, 1–2 drops of solution were added to three-mouth flasks containing buffer solution under magnetic stirring. The feeding speed was controlled to 5 mL·min<sup>-1</sup>, and the reaction temperature was set to 55 °C. Thereafter, the mixture continued to react for 8 h under strong stirring and allowed to age for 10 h at 60 °C.

Ni<sub>0.8</sub>Mn<sub>0.2</sub>(OH)<sub>2</sub> samples coated with CoOOH were prepared by chemical coprecipitation method [23,24], and the cobalt mass fractions were 2.5%, 5%, 7.5% and 10%. Firstly, appropriate amounts of CoSO<sub>4</sub> were dissolved in 200 mL of distilled water on the basis of the quality ratios of Ni and Co at 97.5:2.5, 95:5, 92.5:7.5 and 90:10; thus, solution 4 was prepared. Solution 5 was obtained by dissolving 16 g NaOH in 200 mL of deionised water. Thirdly, 4–5 drops of solution were added simultaneously to a three-mouth flask containing a solution of Ni<sub>0.8</sub>Mn<sub>0.2</sub>(OH)<sub>2</sub> under magnetic stirring. The feeding speed was controlled to 5 mL·min<sup>-1</sup>, and the reaction temperature was set to 55 °C. Thereafter, the mixture continued to react for 8 h under strong stirring and allowed to age for 10 h at 60 °C. The mixture was filtered and washed to neutrality with warm deionised water. The samples were dried in a vacuum drying chamber at 60 °C to a constant weight and then milled in a ball mill at 400 r·min<sup>-1</sup> for 4 h to form powder samples.

The sample, graphite emulsion (alcohol soluble, 30 wt% solid content) and nickel powder were mixed in a 3:1:1 ratio and then added with an appropriate amount of anhydrous alcohol. After grinding for 30 min by an agate mortar, the slurry was coated on 2 cm×2 cm foam nickel. After drying at 60 °C for 4 h, another 2 cm×2 cm foam nickel was used to cover the coating with slurry. The nickel electrode was prepared by compacting it on a powder tablet press at 20 MPa.

## 2.2. Material characterisations

X-ray diffraction (XRD; D/Max-3B, Cu K $\alpha$ ) was conducted to analyse the crystal structures of the Ni<sub>1-x</sub>Mn<sub>x</sub>(OH)<sub>2</sub> samples. The working conditions were as follows:  $\lambda=0.1542$  nm, tube pressure of 40 kV, tube flow of 30 mA, scan rate of 2 degree min<sup>-1</sup> and scanning range of  $2\theta=10^{\circ}$ – $80^{\circ}$ . The surface morphology of Ni<sub>1-x</sub>Mn<sub>x</sub>(OH)<sub>2</sub> was observed by SEM. The working voltage was 2 kV.

## 2.3. Electrochemical measurements

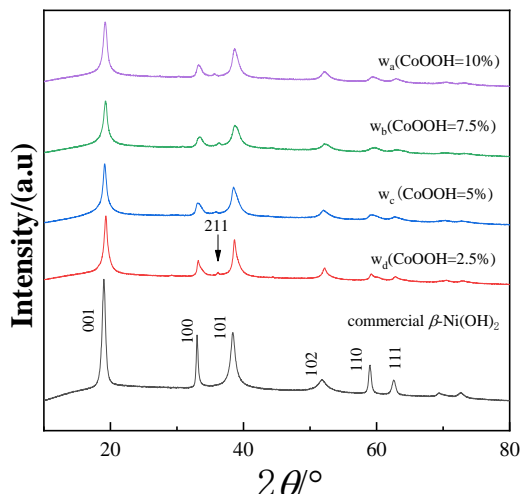
A beaker-type and two-electrode test system was developed with 2 cm $\times$ 2 cm stainless steel strip as negative electrode and 10 mol $\cdot$ L<sup>-1</sup> KOH+1 mol $\cdot$ L<sup>-1</sup> ZnO+20 g $\cdot$ L<sup>-1</sup> LiOH mixed solution as electrolyte. Constant current charging and discharging tests were conducted on the LAND battery test system. The current densities were 100, 150, 200, 300, 500 and 800 mA $\cdot$ g<sup>-1</sup>. The charging cut-off conditions were a capacity of 320 mAh $\cdot$ g<sup>-1</sup> or cut-off voltage of 2.2 V and discharge cut-off voltage of 1.2 V.

A three-electrode test system was constructed using mercury oxide electrode as reference electrode. The cyclic voltammetry (CV) test was conducted at a CHI608E electrochemical workstation. The scan rate was 0.5 mV $\cdot$ s<sup>-1</sup>, and the voltage range was 0–0.7 V (vs. Hg/HgO).

# 3. RESULTS AND DISCUSSION

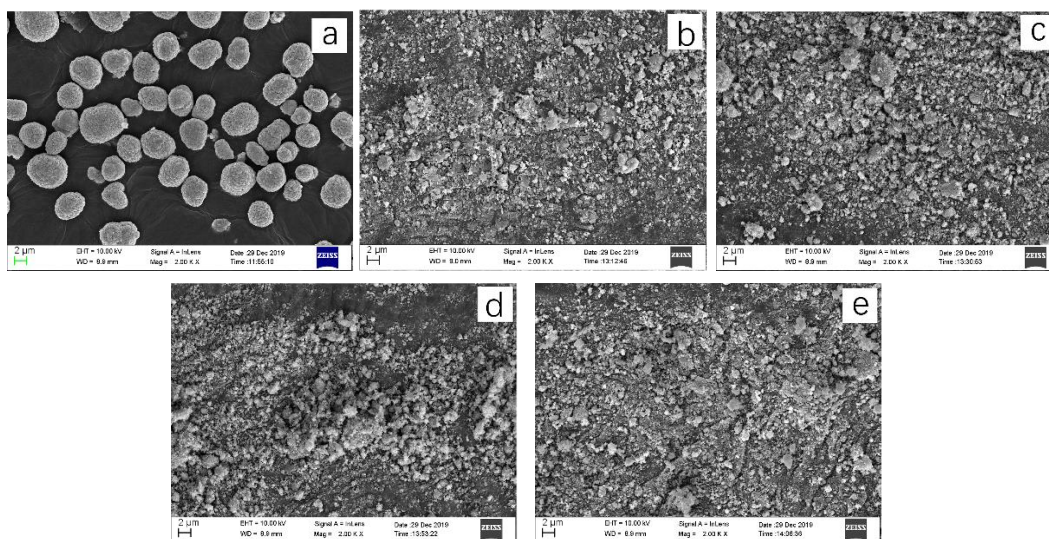
## 3.1 Phase analysis

Fig. 1 shows the XRD patterns of commercial  $\beta$ -Ni(OH)<sub>2</sub> and Ni<sub>0.8</sub>Mn<sub>0.2</sub>(OH)<sub>2</sub> coated with CoOOH (CoOOH=2.5%, 5%, 7.5%, 10%). By comparing the standard chart (PDF14-0117), the diffraction peaks at  $2\theta=19.07^{\circ}$ ,  $33.23^{\circ}$ ,  $38.70^{\circ}$ ,  $52.22^{\circ}$ ,  $59.03^{\circ}$ ,  $62.63^{\circ}$  were observed in the figure. These peaks corresponded to crystal faces (001), (100), (101), (102), (110) and (111). All five samples showed typical  $\beta$ -Ni(OH)<sub>2</sub> structural features, and cobalt coating did not change the crystal structure of Ni(OH)<sub>2</sub>. The diffraction peaks of samples at  $2\theta=35.99^{\circ}$  were consistent with the (211) crystal plane of Mn<sub>3</sub>O<sub>4</sub> (PDF04-0732), which indicated the presence of Mn<sub>3</sub>O<sub>4</sub> impurities, which might be caused by partial oxidation of manganese ion in the sample preparation process. Fig. 1 shows that, as the amount of CoOOH coating decreased, the peak shape became increasingly sharp, and the half-width of CoOOH-coated Ni<sub>0.8</sub>Mn<sub>0.2</sub>(OH)<sub>2</sub> became narrow. According to the X-ray Scherrer formula  $\beta=K\lambda/D\cos\theta$ , the half-width  $\beta$  is inversely proportional to the grain size  $D$  of the powder [25]. The grain size of CoOOH-coated Ni<sub>0.8</sub>Mn<sub>0.2</sub>(OH)<sub>2</sub> gradually increased as the amount of CoOOH coating decreased. The reason was that CoOOH with smaller particle size existed between Ni<sub>0.8</sub>Mn<sub>0.2</sub>(OH)<sub>2</sub> particles, which reduced the average particle size.



**Figure 1.** XRD patterns of commercial  $\beta$ -Ni(OH)<sub>2</sub> and Ni<sub>0.8</sub>Mn<sub>0.2</sub>(OH)<sub>2</sub> coated with CoOOH (CoOOH=2.5%, 5%, 7.5%, 10%).

Fig. 2 shows the SEM images of commercial  $\beta$ -Ni(OH)<sub>2</sub> and Ni<sub>0.8</sub>Mn<sub>0.2</sub>(OH)<sub>2</sub> coated with CoOOH (CoOOH=2.5%, 5%, 7.5%, 10%). As shown in the figures, commercial Ni(OH)<sub>2</sub> was composed of regular spherical particles, and the Ni<sub>0.8</sub>Mn<sub>0.2</sub>(OH)<sub>2</sub> sample particles coated with CoOOH became fine and disorderly due to manganese doping [26]. The porous structure produced by such fine particles could improve contact between the electrolyte and sample, which increased the active material utilisation rate of the sample and improved the electrical properties of the sample. Figs. 2b and 2c show that the coating effect was good, and many fine CoOOH were dispersed amongst the particles, which could enhance the electrical conductivity between the particles. As shown in Figs. 2d and 2e, an obvious agglomeration phenomenon occurred, which was due to the high amount of cobalt coating. CoOOH started to grow in disorder on the surface of particles, which made the coating effect poor.



**Figure 2.** SEM patterns of commercial  $\beta$ -Ni(OH)<sub>2</sub> and Ni<sub>0.8</sub>Mn<sub>0.2</sub>(OH)<sub>2</sub> coated with CoOOH (CoOOH=2.5%, 5%, 7.5%, 10%).

### 3.2 Electrochemical analysis

Fig. 3 shows the CV curves of commercial  $\beta$ -Ni(OH)<sub>2</sub> and Ni<sub>0.8</sub>Mn<sub>0.2</sub>(OH)<sub>2</sub> coated with CoOOH (CoOOH=2.5%, 5%, 7.5%, 10%) at a scan rate of 0.5 mV·s<sup>-1</sup> and a voltage range of 0–0.7 V (vs. Hg/HgO). The curves of the five samples showed a pair of redox peaks, which were consistent with a discharge platform in the constant current charge and discharge curve. The difference  $\Delta E$  between the oxidation and reduction peak potentials reflects the reversibility of the electrochemical reaction; a small  $\Delta E$  indicates good reversibility of the electrode reaction[27]. As shown in Fig. 3,  $\Delta E$  of  $\beta$ -Ni(OH)<sub>2</sub> was 460 mV, and the values for CoOOH-coated samples were 385 mV (CoOOH=2.5%), 340 mV (CoOOH=5%), 450 mV (CoOOH=7.5%) and 410 mV (CoOOH=10%). Therefore, the electrode had good reversible property after coating CoOOH. In addition, the oxygen evolution potential of Ni<sub>0.8</sub>Mn<sub>0.2</sub>(OH)<sub>2</sub> coated with CoOOH was significantly increased, and the difference between the oxygen evolution potential and the oxidation peak potential of Ni<sub>0.8</sub>Mn<sub>0.2</sub>(OH)<sub>2</sub> sample was the largest when CoOOH=5%. When the difference between oxygen evolution potential and oxidation peak potential was larger, the oxygen evolution would be less when the electrode was charged[17]. Thus, the active substance utilisation rate of samples with a CoOOH mass fraction of 5% was higher.

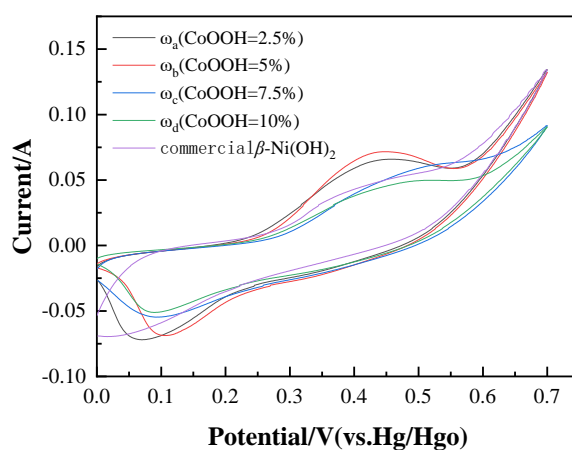


**Figure 3.** CV curves of commercial  $\beta$ -Ni(OH)<sub>2</sub> and Ni<sub>0.8</sub>Mn<sub>0.2</sub>(OH)<sub>2</sub> coated with CoOOH at scan rate of 0.5 mV·s<sup>-1</sup> (CoOOH=2.5%, 5%, 7.5%, 10%).

Fig. 4 is a charge and discharge curve cycle of commercial Ni(OH)<sub>2</sub> and Ni<sub>0.8</sub>Mn<sub>0.2</sub>(OH)<sub>2</sub> coated with CoOOH at a current density of 100 mA·g<sup>-1</sup> (CoOOH=2.5%, 5%, 7.5%, 10%). At this point, the specific discharge capacity of the sample was stable. The discharge specific capacity of commercial  $\beta$ -Ni(OH)<sub>2</sub> was 265 mAh/g, whilst the discharge specific capacities of sample coated with CoOOH were 273 mAh/g (CoOOH=2.5%), 278 mAh/g (CoOOH=5%), 255 mAh/g (CoOOH=7.5%) and 239 mAh/g (CoOOH=10%). The figure also shows that the charging platform of the sample was the lowest when the mass fraction of the coated CoOOH was 5%. The charging and discharging platform was inversely proportional to the charging efficiency. The sample with a CoOOH mass fraction of 5% had the highest charging efficiency due to the increased electrical conductivity between particles coated with

CoOOH[28]. In addition, sample CoOOH=5% had a higher discharge platform, which indicated that the sample had a higher discharge specific capacity. The reasons for the emergence of a second discharge platform in the sample were twofold. On the one hand, it was related to the positive pole. When the electrode overdischarged, Co and Mn discharged at low potential; on the other hand, the loosening of the contact between the sample and nickel foam caused the drop of the voltage platform [20].

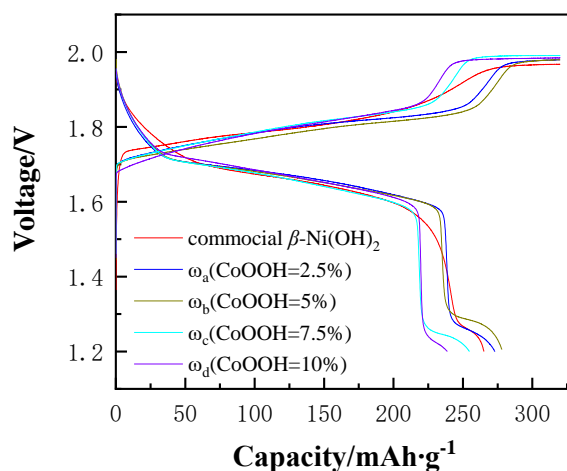


**Figure 4.** Charge–discharge curves of commercial  $\beta$ -Ni(OH)<sub>2</sub> and Ni<sub>0.8</sub>Mn<sub>0.2</sub>(OH)<sub>2</sub> coated with CoOOH at a current density of 100 mA·g<sup>-1</sup> (CoOOH=2.5%, 5%, 7.5%, 10%).

Fig. 5 shows the rate performance of commercial  $\beta$ -Ni(OH)<sub>2</sub> and Ni<sub>0.8</sub>Mn<sub>0.2</sub>(OH)<sub>2</sub> coated with CoOOH at current densities of 150, 200, 300 and 500 mA·g<sup>-1</sup>. Tab. 1 shows the comparison of discharge specific capacity of different electrode materials. As shown in Fig. 5, the discharge specific capacity of each sample reached the highest at low current density, and sample CoOOH=5% had a discharge specific capacity of 282 mAh/g. The specific discharge capacity of sample CoOOH=2.5% was 278 mAh/g, which was slightly lower than that of sample CoOOH=5%. The discharge specific capacities of samples commercial  $\beta$ -Ni(OH)<sub>2</sub>, CoOOH=7.5% and CoOOH=10% were lower at 270, 255 and 239 mAh/g, respectively. When the current density increased from 150 mA·g<sup>-1</sup> to 500 mA·g<sup>-1</sup>, the discharge specific capacity of the sample CoOOH=5% was larger than that of the sample CoOOH=2.5%. Moreover, the cyclic stability of the sample CoOOH=2.5% was poor, and the discharge specific capacity of the sample CoOOH=5% decreased greatly at current density of 150 mA·g<sup>-1</sup>. The discharge specific capacities of samples CoOOH=7.5% and CoOOH=10% were lower than that of commercial  $\beta$ -Ni(OH)<sub>2</sub>, but the performance of charge and discharge cycle was relatively stable at various current densities. With the increase in the current density, the samples coated with CoOOH showed better stable performance in charge and discharge cycle. However, the specific discharge capacity of each sample showed a trend of gradual decrease. The specific discharge capacity decreased with the increase in current density. The reason was that the redox reaction was not completed due to the increase in partial pressure on the electrode resistance [29].

**Table 1.** Comparison of discharge specific capacity of different electrode materials

References	Electrode materials	Preparation method	discharge specific capacity/ mAh/g
this work	CoOOH- coated Ni <sub>0.8</sub> Mn <sub>0.2</sub> (OH) <sub>2</sub>	A chemical coprecipitation	282
X. G. Hou [14]	CoOOH-coated β-Ni(OH) <sub>2</sub>	precipitation transformation	288
P. Xia [15]	Co-coated α-Ni(OH) <sub>2</sub>	A chemical coprecipitation	358.6
W. X. Hao [16]	Co(OH) <sub>2</sub> -Yb(OH) <sub>3</sub> -coated β-Ni(OH) <sub>2</sub>	A chemical coprecipitation	292
X. M. He [17]	Yb/Co-coated Ni(OH) <sub>2</sub>	A chemical coprecipitation	281
W. Li[18]	Yb(OH) <sub>3</sub> -coated Ni(OH) <sub>2</sub>	Controlled crystallization method	270
X. Lv [19]	CoOOH-coated β-Ni(OH) <sub>2</sub>	A chemical coprecipitation	243

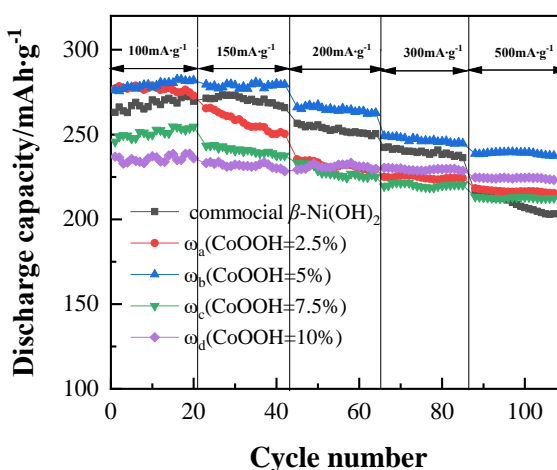


**Figure 5.** Rate performance of commercial β-Ni(OH)<sub>2</sub> and Ni<sub>0.8</sub>Mn<sub>0.2</sub>(OH)<sub>2</sub> coated with CoOOH (CoOOH=2.5%, 5%, 7.5%, 10%).

Fig. 6 shows the cyclic performance of commercial β-Ni(OH)<sub>2</sub> and Ni<sub>0.8</sub>Mn<sub>0.2</sub>(OH)<sub>2</sub> coated with CoOOH (CoOOH=2.5%, 5%, 7.5%, 10%) at 800 mA·g<sup>-1</sup>. As shown in Fig. 6, the CoOOH-coated sample presented better discharge performance and a higher discharge specific capacity than β-Ni(OH)<sub>2</sub>. The maximum discharge specific capacity of the β-Ni(OH)<sub>2</sub> sample was 194 mAh·g<sup>-1</sup>, and the maximum discharge specific capacity of the sample CoOOH=5% was 234.5 mAh·g<sup>-1</sup>.

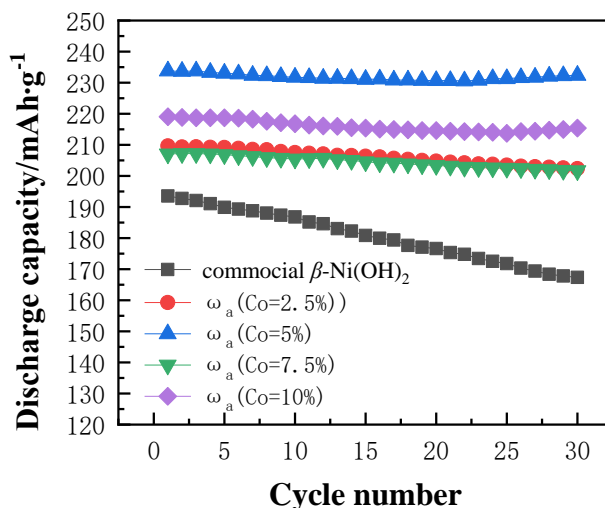


**Figure 6.** Cyclic performance of commercial  $\beta$ -Ni(OH)<sub>2</sub> and Ni<sub>0.8</sub>Mn<sub>0.2</sub>(OH)<sub>2</sub> coated with CoOOH at 800 mA·g<sup>-1</sup> (CoOOH=2.5%, 5%, 7.5%, 10%).

The electrodes of Ni<sub>0.8</sub>Mn<sub>0.2</sub>(OH)<sub>2</sub> with different CoOOH contents showed a relatively stable cycle life. After 30 cycles, the discharge specific capacity of commercial  $\beta$ -Ni(OH)<sub>2</sub> decreased by 11.5%. The other samples were attenuated by 3.3% (CoOOH=2.5%), 3% (CoOOH=7.5%) and 1.4% (CoOOH=10%). When CoOOH=2.5%, the discharge specific capacity of the samples did not decrease. Thus, CoOOH could effectively improve the discharge performance and cycle stability of the nickel electrode after coating CoOOH. The CoOOH coating increased the charge transfer between the particles and inhibited the polarisation of the electrode. In addition, the CoOOH coating inhibited the production of  $\gamma$ -NiOOH, and  $\gamma$ -NiOOH resulted in electrode expansion and decreased electrode life[30].

#### 4. CONCLUSIONS

Ni<sub>0.8</sub>Mn<sub>0.2</sub>(OH)<sub>2</sub> (CoOOH=2.5%, 5%, 7.5%, 10%) cathode materials coated with different contents CoOOH were prepared by chemical coprecipitation method. The morphological characteristics and electrochemical properties of Ni<sub>0.8</sub>Mn<sub>0.2</sub>(OH)<sub>2</sub> coated with CoOOH were studied, and the following conclusions were drawn.

(1) XRD analysis showed that the Ni<sub>0.8</sub>Mn<sub>0.2</sub>(OH)<sub>2</sub> coated with CoOOH samples were all  $\beta$  phase, the samples CoOOH=2.5%, 5%, 7.5%, 10% showed a heterogeneous phase and the CoOOH-coated samples presented a narrow half-width and fine grains.

(2) The SEM test revealed that the CoOOH-coated sample was finer than the commercial  $\beta$ -Ni(OH)<sub>2</sub> particles, and CoOOH attachment on the surface of the samples was observed.

(3) The CV test showed that the difference between the oxidation the reduction peak potentials of the CoOOH-coated sample was small, and the electrode reversibility was good. The oxygen evolution potential of the electrode was increased, and the utilisation rate of the active substance was increased.

(4) The discharge specific capacity of the CoOOH-coated sample increased firstly and then decreased with the increase in the CoOOH content. When CoOOH=5%, the sample had a discharge

specific capacity of  $282 \text{ mAh}\cdot\text{g}^{-1}$  at a current density of  $100 \text{ mA}\cdot\text{g}^{-1}$ , and the discharge specific capacity of commercial  $\beta\text{-Ni(OH)}_2$  under the same conditions was  $270 \text{ mAh}\cdot\text{g}^{-1}$ . These results showed that coating CoOOH could increase the discharge specific capacity of nickel electrode and improve its current charge and discharge performance.

(5) When CoOOH=5%, the sample showed good cycle stability. The sample was circulated for 30 cycles under the same conditions. The discharge specific capacity was not attenuated when CoOOH=5%, whereas the commercial  $\text{Ni(OH)}_2$  was attenuated by 11.5%. The other samples were attenuated by 3.3% (CoOOH=2.5%), 3% (CoOOH=7.5%) and 1.4% (CoOOH=10%).

#### ACKNOWLEDGEMENTS

The authors acknowledge the financial support from the National Natural Science Foundation of China (No. 51776092).

#### References

1. Y. -S. Yang, L. Zhang, Y. -H. Wen, J. Cheng, G. -P. Cao, *Chin. J. Power Sources*, 03(2007)175. J. Cheng, L. Zhang, Y. -S. Yang, Y. -H. Wen, G. -P. Cao, X. -D. Wang, *Electrochem. Commun.*, 9(2007)2639.
2. L. Zhang, J. Cheng, Y. -S. Yang, Y. -H. Wen, X. -D. Wang, G. -P. Cao, *J. Power Sources*, 179(2008)381.
3. J. Cheng, Y. -H. Wen, G. -P. Cao, Y. -S. Yang, *J. Power Sources*, 196(2011)1589.
4. Y. -X. Wang, Z. -A. Hu, H. -Y. Wu, *Mater. Chem Phys.*, 126(2011)580.
5. Q. Zhang, Y. -H. Xu, X. -L. Wang, *Mater. Chem Phys.*, 86(2004)293.
6. G. -H. Liu, Y. -G. Li, A. Chen, C. -S. Huang, *Guangdong. Chem Ind.*, 43(2016)57. X. -H. Wu, Q. -P. Feng, M. Wang, G. -W. Huang, *J. Power Sources*, 329(2016)170.
7. C. -C. Miao, Y. -J. Zhu, L. -G. Huang, T. -Q. Zhao, *Ionics*, 21(2015)2295.
8. X. -F. Li, S. -Y. Li, T. -C. Xia, *Zhengzhou Univ. Light Ind. (Nat. Sci. Ed.)*, 24(2009)16. W. -X. Hao, Y. -Q. Zhang, W. -Q. Jiang, Z. -Z. Fu, L. -M. Yu, W. -G. Zhang, *B. Chin Ceram Soc.*, 27(2008)276.
9. H. -M. Deng, *Shanxi Metall*, 37(2014)14.
10. J. -M. Chen, J. -T. Sun, Y. -H. Song, *J. Synthetic Cryst.*, 45(2016)1539. X. -G. Hou, W. -W. Liu, C. -X. Li, Y. -F. Wang, X. -F. Wang, *J. Lanzhou Univ. Techno.*, 39(2013)10. P. Xia, J. Yang, B. -J. Deng, S. -Q. Zhao, G. -F. Yu, B. -R. Zhan, H. -B. Zhou, X. -L. Ge, *J. Hubei Univ. Eng.*, 35(2015)83.
11. W. -X. Hao, S. -L. An, Y. -Q. Zhang, W. -Q. Jiang, *Rare Met. Mater. Eng.*, 41(2012)1129. X. -M. He, C. -Y. Jiang, W. Li, C. -R. Wan, *Rare Met. Mater. Eng.*, 36(2007)291. W. Li, C. -Y. Jiang, C. -R. Wan, *J. Inorg. Mater.*, 21(2006)121. X. Lv, G. Xie, X. -C. He, Y. -Q. Hou, X. -H. Yu, *Chin. J. Power Sources*, 42(2018)1889. M. Xiao, R. -Y. Xing, S. -G. Yao, J. Cheng, Y. -J. Shen, Y. -S. Yang, *J. Inorg. Mater.*, 34(2019)703.
12. Y. Li, Y. -S. Xie, J. -H. Gong, Y. -F. Chen, Z. -T. Zhang, *Mater. Sci. Eng. B*, 86(2001)119.
13. S. -G. Yao, R. -Y. Xing, J. Cheng, M. Xiao, *Bat. Bim.*, 49(2019)182.
14. X. -Z. Qin, G. Yang, J. Gao, F. -P. Cai, B. Wang, B. Jiang, C. -H. Tan, *Shandong Sci*, 30(2017)43. L. -F. Xia, L. -J. Li, H. -P. Yang, Z. -X. Zhao, *Min. Metall. Eng.*, 40(2020)123.
15. X. -B. Ben, M. -X. -Z. Duan, *Semiconductor Techno*, 44(2019)115. S. -G. Yao, F. Dou, R. -Y. Xing, J. Cheng, M. Xiao, *Chinese. J. Inorg. Chem.*, 35(2019)1403. C. -C. Zhang, C. Xin, D. -H. Xu, *Appl Surf Sci.*, 428(2018)73.

16. D. Guo, E. -B. Shangguan, J. Li, T. -H. Zhao, Z.-R. Chang, Q. -M. Li, *Int J Hydrogen Enegr.*, 39(2014)3895.
17. X. -S. Li, W. -X. Hao, Y. -Q. Zhang, J. Meng, H. -Y. Yu, *J. Funct. Mater.*, 47(2016)8200. Z. -R. Chang, B. Li, Y. -P. Li, X. -J. Wei, *Chin. J Appl Chem.*, 20(2003)360.

© 2021 The Authors. Published by ESG ([www.electrochemsci.org](http://www.electrochemsci.org)). This article is an open access article distributed under the terms and conditions of the Creative Commons Attribution license (<http://creativecommons.org/licenses/by/4.0/>).